A Simplified Model of Phase Evolution in Comb-based Time-frequency Transfer

Dongrui Yu, Yufei Zhang, Ziyang Chen, Hong Guo*
State Key Laboratory of Advanced Optical Communication Systems and Networks
School of Electronics, and Center for Quantum Information Technology, Peking University
Beijing, China
hongguo@pku.edu.cn

***Abstract*—Optical frequency combs, characterized by high signal-to-noise ratio and fine time resolution, have made significant contributions in the field of optical time-frequency transfer towards long distance and high precision. In such a system, the phase time information of the combs is hard to directly describe, which set barriers to further improving the system performance via theoretical analysis. In this work, we present a simplified model of comb phase evolution in fiber, based on coherent wave superposition, to quantitatively characterize the phase time variation. The impact of OFC repetition frequency fluctuation, carrier-envelope-offset fluctuation and dispersion terms during propagation are analyzed respectively, and numerical simulations can further simplify and visualize the calculations. Future optimization is expected to involve self-phase modulation and other nonlinear effects.**

***Index Terms*—OFC, TFT, phase evolution, model**

I. Introduction

In recent years, with the help of the high signal-to-noise ratio (SNR) and short pulse width characteristics of the optical frequency combs (OFCs), the OFC-based optical time-frequency transfer (O-TFT) has made a large step towards long distance and high precision [1]–[3], which is the persistent obsession of this field. The frequency transfer distance has reached 3000 km [4], and the time-interval-measurement precision has arrived the femtosecond (fs, 1 fs = 10^{-15} s) level [5]. In the field of optical time-frequency transfer, fractional frequency instability is the key indicator, which is ultimately determined by the phase time fluctuation of the signals. Consequently, phase time is the element to be measured, manipulated, and analyzed in the experiment. While the phase time information of the OFCs is hard to be directly modeled and calculated via solving the nonlinear Schrödinger (NLS) equation (i.e., the common approach to the OFC propagation problems) since it focuses on the envelope shape evolution of the comb pulses [6].

In this work, a simplified model of OFC phase evolution is presented based on coherent wave superposition, considering the technical noise types and fiber dispersion, to quantitatively characterize the phase-related parameters. This model enables various analyses, including assessing the impact of carrier-envelope-offset frequency and repetition frequency fluctuations on the detected pulse phase, evaluating pulse shape variations induced by the fiber dispersion, as well as analyzing the frequency-dispersion coupling terms. Numerical simulations are also performed to visualize the impact from different elements on the pulse shape and phase time.

II. Model Establishment & Results

The simplified model of OFC phase evolution in the O-TFT system is developed from the aspects of anti-Fourier transform of the OFC's spectrum,

$$B(t) = \frac{1}{2\pi}\int_{-\infty}^{+\infty} \tilde{B}(\omega)\exp(-j\omega t)\mathrm{d}\omega, \tag{1}$$

where $\tilde{B}(\omega)$ is the spectrum of the OFC signal. In the traditional means to describe the OFC-propagation-in-fiber (i.e., the NLS equation), the quasi-monochromatic wave approximation and the slow-varying envelope approximation are considered and the fast-oscillating term $\exp(-j\omega t)$ is separated with the envelope amplitude

$$A(t) = \frac{1}{2\pi}\int_{-\infty}^{+\infty} \tilde{B}(\omega)\mathrm{d}\omega, \tag{2}$$

whose evolution could be described by solving the NLS equation.

In this work, the discrete-comb-teeth approximation in the frequency domain is considered and (1) can be rewritten as

$$B(t) = \sum_{n=0}^{N-1} B_n \exp[-j(\omega_0 + n\omega_{\text{rep}})t], \tag{3}$$

where B_n is the amplitude of the n^{th} comb tooth, ω_0 is the angular frequency of the lowest-frequency comb tooth in the spectrum, and ω_{rep} is the repetition angular frequency of the OFC. It is worth noting that ω_0 is determined by the carrier-envelope-offset angular frequency ω_{CEO} by

$$\omega_0 = \omega_{\text{CEO}} + M\omega_{\text{rep}}, \tag{4}$$

where M is a large integer that ensures ω_0 in the optical region.

Considering the OFC-induced noise and fiber dispersion in the O-TFT system, (3) can be expanded to

$$B(z, t-\tau) = \sum_{n=0}^{N-1} B_n \exp\left\{-j(\omega_0 + n\omega_{\text{rep}})(t-\tau) - j\int_0^{t-\tau} \left[\delta\omega_0(t') + n\delta\omega_{\text{rep}}(t')\right]\mathrm{d}t' + j\beta z\right\}. \tag{5}$$

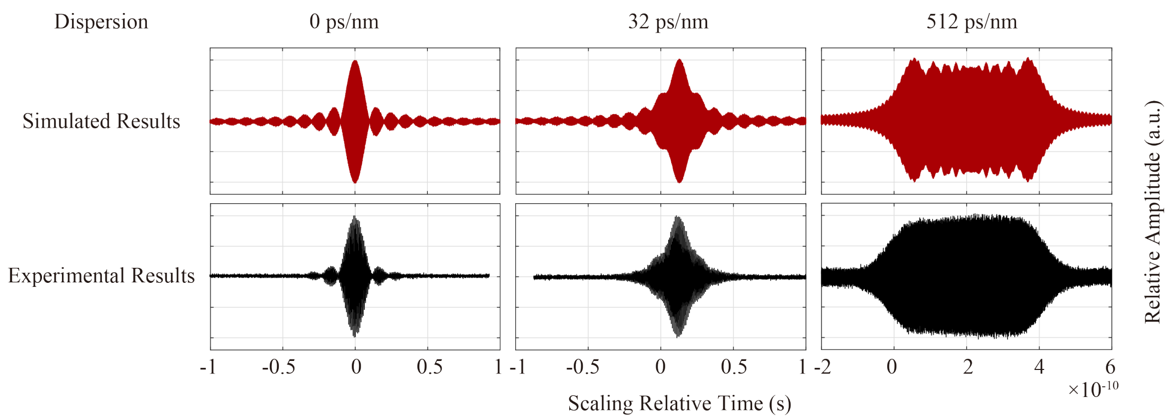

Fig. 1. Simulated pulse broadening versus experimentally acquired result.

In (5), τ is the initial signal delay, $\delta\omega_i(t)$ denote the frequency fluctuation of ω_0 and ω_{rep} respectively, β is the mode-propagation constant, and z is the propagation distance. Equation (5) is the simplified model of the OFC signal in the O-TFT system, which would provide clear results and conclusions in the specific experimental conditions below.

A. Direct photodetection of the OFC signal

In the field of O-TFT, evaluating and utilizing the frequency signal both need to convert the optical signal into electrical ones via photodetection. Considering the fact that the photodetection process detects the signal power and has a bandwidth limit (BW), the detected comb signal can be denoted as

$$\begin{aligned} &I(t-\tau) \\ &= \sum_{l=m-n,\ \frac{l\omega_{\text{rep}}}{2\pi}<\text{BW}} B_l' \exp\left\{-jl\omega_{\text{rep}}[t-\tau+x_{\delta\omega_{\text{rep}}}(t-\tau)]\right\}, \end{aligned} \tag{6}$$

where

$$x_{\delta\omega_{\text{rep}}}(t) = \frac{1}{\omega_{\text{rep}}}\int_0^t \delta\omega_{\text{rep}}(t')\text{d}t' \tag{7}$$

is the repetition-frequency-fluctuation-induced phase time variation. It is clearly shown in (6) that the phase time of the OFC signal, which has the dimension of [s], is composed of two terms, the initial signal delay τ and the repetition-frequency-related fluctuation. The ω_0-related terms have no contribution to the signal phase time.

This result is consistent with previous works that utilized OFCs as the carrier of O-TFT. In the early-stage publications, the CEO frequencies of the OFCs are manually stabilized. As an example, in 2005, JILA (the Joint Institute for Laboratory Astrophysics, NASA) realized the frequency transfer with the instability of 9×10^{-15} @ 1 s in a 7 km fiber link [7]. In the late-stage works, the CEO frequencies of the OFCs are all free-running, and it did not affect the steps of OFC-based O-TFT towards longer distances and better stability. For instance, the work of NPL (National Physical Laboratory) in 2010 realized frequency transfer instability of 5×10^{-15} @ 1 s in a 50 km fiber link [8].

This simplified model gives a result and explanation about the unnecessity of stabilization of the CEO frequency in the short-distance frequency transfer experiments.

B. Photodetection of the transferred OFC signal

For longer transfer distances, e.g., over hundreds of kilometers, the dispersion-induced effects cannot be ignored. The photodetection result of (5), considering the propagation, is

$$\begin{aligned} &I(t-\tau, z) \\ &= \sum_{\frac{(m-n)\omega_{\text{rep}}}{2\pi}<\text{BW}} B_{mn}' \exp\{-j(m-n)\omega_{\text{rep}} \times \\ &\quad [t-\tau-\beta_1 z && \text{(term A)} \\ &\quad + \frac{1}{\omega_{\text{rep}}}\int_0^{t-\tau} \delta\omega_{\text{rep}}(t')\text{d}t' && \text{(term B)} \\ &\quad - \frac{m+n}{2}\beta_2 z\left(\omega_{\text{rep}} + \delta\omega_{\text{rep}}(t-\tau)\right) && \text{(term C)} \\ &\quad - \beta_1 z \delta\omega_{\text{rep}}(t-\tau)/\omega_{\text{rep}} && \text{(term D)} \\ &\quad - \beta_2 z \delta\omega_0(t-\tau)]\}, && \text{(term E)} \end{aligned} \tag{8}$$

where the high-order fluctuation ($\delta\omega^2$) terms are omitted. In (8), BW is the bandwidth of the photodetector; term A stands for the initial signal delay and the propagation-induced delay; term B describes the pulse broadening caused by second-order dispersion; term C is the repetition-frequency-related phase time fluctuation; term D is the β_1-$\delta\omega_{\text{rep}}$ coupling term; and term E is the β_2-$\delta\omega_0$ coupling term. There are 3 new items in comparison with the directly-detected result (6), which will be further discussed below.

a) Term C: Pulse broadening: In (8), the pulse broadening (term C) is reflected by the inconsistent phase time of different frequency components (indicated by m and n),

$$-\frac{m+n}{2}\beta_2 z\left[\omega_{\text{rep}} + \delta\omega_{\text{rep}}(t-\tau)\right]. \tag{9}$$

The exact phase time is unable to be given, while the pulse shape evolution can be clearly shown by the simulation result using (5), see Fig. 1.

In Fig. 1, the simulated result is obtained by setting $N = 1000$, which corresponds to a single wavelength division multiplexer (WDM) channel; B_n is a constant,which corresponds to a rectangular spectrum; $\tau = 0$ and $\beta_2 z = 0, 32, 512$ ps/nm, respectively. The result is normalized. When $\beta_2 z = 0$, the pulse shape matches a sinc function whose full-width-half-maximum (FWHM) is approximately 20 ps, which is consistent with the anti-Fourier transform of a rectangular function. As the dispersion increases to 32 ps/nm, the pulse shape gradually broadens. When $\beta_2 z = 512$ ps/nm, the FWHM reaches 400 ps, and the pulse shape broadens to a trapezium. The experimentally acquired data is shown in the lower part of Fig. 1, which is obtained with the help of the linear optical sampling (LOS) technique [5]. The OFC signal is streched by

$$\alpha = \frac{f_{\text{rep}}}{\Delta f_{\text{rep}}} = \frac{100\ \text{MHz}}{1\ \text{kHz}} = 10^5 \tag{10}$$

times in the time domain, which can be easily detected and acquired by a balanced photodetector and a oscilloscope, who have the giga Hertz (GHz) level bandwidth and sampling rate. The experimental and simulated results show well consistency in both the pulse shape and the pulse width.

b) Term D: β_1-$\delta\omega_{rep}$ coupling: After being transferred in fiber, the OFC repetition frequency fluctuation induces additional phase noise by coupling with the fiber first-order dispersion [term D in (8)],

$$x_{\beta_1\text{-}\delta\omega_{\text{rep}}} = -\beta_1 z \delta\omega_{\text{rep}}(t - \tau)/\omega_{\text{rep}}. \tag{11}$$

The magnitude of this term could be estimated by comparing it with (7),

$$\frac{x_{\beta_1\text{-}\delta\omega_{\text{rep}}}}{x_{\delta\omega_{\text{rep}}}} = \frac{\beta_1 z \delta\omega_{\text{rep}}/(t)\omega_{\text{rep}}}{\int_0^t \delta\omega_{\text{rep}}(t')\mathrm{d}t'/\omega_{\text{rep}}} = \frac{z \times n}{c} \frac{\delta\omega_{\text{rep}}(t)}{\int_0^t \delta\omega_{\text{rep}}(t')\mathrm{d}t'}, \tag{12}$$

where the first term zn/c is the signal propagation time in fiber, and the second term has the order of 1 if $\delta\omega_{\text{rep}}$ is white noise and has no drift. So only if the propagation time is far larger than 1 s, can the $x_{\beta_1\text{-}\delta\omega_{\text{rep}}}$ term be a major contribution compared to $x_{\delta\omega_{\text{rep}}}$. It requires the total fiber length much longer than 200,000 km, which has far not been achieved (the longest OFC transfer distance is 3000 km [4]). Consequently, the β_1-$\delta\omega_{\text{rep}}$ coupling term is always a non-dominant source of OFC phase time fluctuation.

c) Term E: β_2-$\delta\omega_0$ coupling: A major difference between the transferred and non-transferred OFC signal is the term E in (8), which reflects the phase time fluctuation brought by $\delta\omega_0$. In the non-transferred situation, the $\delta\omega_0$ has no impact on the photodetected signal phase time (Sec. II-A), while in the transferred situation, $\delta\omega_0$ couples with the fiber second-order dispersion and brings the term E in (8),

$$x_{\beta_2\text{-}\delta\omega_0} = -\beta_2 z \delta\omega_0(t - \tau). \tag{13}$$

To clearly show the phase time variation brought by the β_2-$\delta\omega_0$ coupling, another simulation is performed (Fig. 2). It shows a 0.1 ps phase time difference originate from a $\delta\omega_0 = 2\pi\times50$ MHz difference, when the OFC signal is transferred through a 100 km comercial fiber. The pulse proadening is serious and only part of the pulse is exhibited.

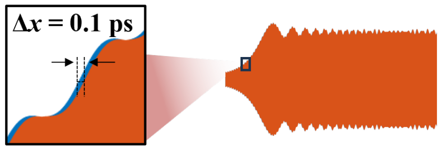

Fig. 2. Simulated β_2-$\delta\omega_0$-coupling-induced phase time variation. The red and blue signal have a ω_0 difference of $2\pi\times50$ MHz, and they are simulated to be transferred through a 100 km comercial fiber.

It is worth noting, in real long-distance OFC transfer experiments, distributed dispersion compensation is generally utilized to compensate the pulse broadening. Meanwhile, the β_2-$\delta\omega_0$ coupling term can also be compensated and does not have any influence on the phase time. However, under certain conditions where the dispersion cannot be accurately compensated, the influence raised by the coupling term still needs to be evaluated.

III. Conclusion and Discussion

In this work, we demonstrate a simplified signal model that can directly describe the phase evolution of OFC signals in a O-TFT system. Based on this model, some results that have reference value are produced, e.g. the unnecessity of locking f_{CEO} in a OFC-based O-TFT experiment, and the phase nosie source in such a system. To further optimize the signal model, the non-linearities and higher-order dispersion would be the next steps, which might provdide more accurate description of the phase noise and pulse evolution.

Acknowledgment

This work was supported by China Postdoctoral Science Foundation (2020TQ0016); National Natural Science Foundation of China (61531003, 62201012).

References

[1] K. Y. Jung, J. Shin, J. Kang, S. Hunziker, C. K. Min, and J. Kim, “Frequency comb-based microwave transfer over fiber with 7×10^{-19} instability using fiber-loop optical-microwave phase detectors,” Opt. Lett., vol. 39, pp. 1577-80, 2014.

[2] X. Chen *et al.*, “Simultaneously precise frequency transfer and time synchronization using feed-forward compensation technique via 120 km fiber link,” Sci. Rep., vol. 5, p. 18343, 2015.

[3] C. Qian, C. Wang, S. Li, and J. Zhao, “Precise radio frequency dissemination via simulated 3000-km fiber re-circulating loop,” IEEE Photon. Tech. Lett., vol. 29, pp. 1572-1575, 2017.

[4] D. Yu *et al.*, “Microwave frequency transfer over 3000-km fiber based on optical frequency combs and active noise cancellation,” Phys. Rev. Res., vol. 6, p. 023005, 2024.

[5] D. Yu *et al.*, “Time interval measurement with linear optical sampling at the femtosecond level,” Photon. Res., vol. 11, pp. 2222-2230, 2023.

[6] G. P. Agrawal, P. L. Christiansen, M. P. Sørensen, and A. C. Scott, Eds. Nonlinear Fiber Optics. Berlin, Heidelberg: Springer Berlin Heidelberg, 2000.

[7] K. W. Holman, D. D. Hudson, J. Ye, and D. J. Jones, “Remote transfer of a high-stability and ultralow-jitter timing signal,” Opt. Lett., vol. 30, pp. 1225-1227, 2005.

[8] G. Marra, H. S. Margolis, S. N. Lea, and P. Gill, “High-stability microwave frequency transfer by propagation of an optical frequency comb over 50 km of optical fiber,” Opt. Lett., vol. 35, pp. 1025-1027, 2010.